

# Reservoir Fluid Replacement Modeling of Acoustic Impedance Module by Machine Learning.

<sup>1</sup>Akindeji Opeyemi Fajana, <sup>1</sup>Emeka Christian Azika.

<sup>1</sup>Department of Geophysics, Faculty of Science,  
Federal University Oye-Ekiti, Ekiti State, Nigeria.

<sup>1\*</sup>Corresponding email: [akindeji.fajana@fuoye.edu.ng](mailto:akindeji.fajana@fuoye.edu.ng)

## Abstract

This study focuses on the modeling of acoustic impedance in reservoir fluids during the process of fluid replacement. Acoustic impedance is a crucial parameter for characterizing subsurface formations and plays a vital role in various applications, including reservoir characterization and hydrocarbon exploration. Understanding the changes in acoustic impedance during fluid replacement can provide valuable insights into the fluid distribution and reservoir properties. Integration of machine learning (ML) techniques with reservoir fluid replacement modeling to enhance the prediction of acoustic impedance, is a critical step in reservoir characterization. In this study, fluid dynamics and reservoir behavior in conventional and non-conventional reservoir systems are meticulously analyzed using two models: a Conventional Reservoir (Model 1) and a Shally/Non-Conventional Reservoir (Model 2). Three different scenarios (Cases 1, 2, 3) involving brine, oil, and gas are considered. Notable variations in initial and final compressional and shear velocities and combined bulk modulus values are observed in both models. In each case, constancy in a specific fluid parameter is maintained, despite changes in other parameters, which implies the existence of an intrinsic feedback mechanism striving for equilibrium within the system. A reduction in both compressional and shear velocities, alongside an increase in the bulk modulus, is noticed, indicating a distinctive system response to fluid extraction. Changes in the bulk modulus suggest an adaptation of the reservoir system to uphold its structural integrity, despite the decrease in fluid volume. In the non-conventional model, a decline from initial to final values in compressional and shear moduli is witnessed, implying an increased potential for deformation and a decreased ability of the reservoir to withstand stresses. In contrast, an ascension in the combined bulk modulus values indicates the reservoir's resilience in withstanding external pressure forces. Additionally, the study reveals the differential effects of various fluids on acoustic impedance, with a reduction induced by the gas being particularly noteworthy. A complex interplay of fluid states leading to significant influence on hydrocarbon density is also unraveled, which offers key insights into the reservoir's potential. The importance of understanding the intricate relationships between temperature, pressure, and entropy in defining fluid phases within reservoir systems is emphasized. Finally, the significant role of lithological factors, often surpassing the effects of fluids on reservoir behavior, is highlighted. The comprehensive understanding of reservoir dynamics brought forward by this study could serve as a guide for the development of more efficient extraction strategies and sustainable reservoir management practices.

**Keywords:** reservoir characterization, hydrocarbon exploration, bulk modulus, lithological factors

## Article Highlights

1. The research investigates fluid dynamics and behaviour in conventional and unconventional (Shally) reservoirs. It found that in conventional reservoirs, fluid parameters (brine, oil, and gas) behave predictably. However, in unconventional reservoirs, fluid behaviours are more complex and dependent on specific conditions.

2. In both types of reservoirs, as fluid extraction occurs, there's a decrease in the reservoir's ability to transmit pressure changes (compressional and shear velocities), and an increase in the reservoir rock's resistance to volume changes (bulk modulus). This could be a response to maintain reservoir structural integrity during fluid extraction.

3. These findings have important implications for reservoir management and hydrocarbon extraction strategies. Understanding these behaviours can inform more efficient and sustainable extraction strategies, aiding in better management and exploitation of the reservoirs, and fostering advancements in reservoir science and technology.

### 1.1 Introduction

The characterization of subsurface reservoirs and their fluid properties is essential for efficient hydrocarbon exploration and production. Acoustic impedance, a property derived from the density and velocity of the subsurface medium, is a key parameter in reservoir characterization studies. It provides valuable information about lithology, porosity, fluid content, and structural features of the reservoir. Acoustic impedance has proven to be a reliable tool for identifying fluid-bearing zones and evaluating the potential of hydrocarbon reservoirs.

Acoustic impedance ( $Z$ ) is defined as the product of the density ( $\rho$ ) and the acoustic velocity ( $V$ ) of the medium through which sound waves propagate. It represents the resistance offered by the medium to the transmission of sound waves. Acoustic impedance is commonly measured in units of rayls ( $\text{kg/m}^2\text{s}$ ). In the context of reservoir geoscience, acoustic impedance is an important parameter as it aids in the discrimination of different fluid types and rock formations based on their respective acoustic responses.

Fluid replacement refers to the process of substituting one fluid phase within a reservoir with another. The change in fluid properties during this process can significantly alter the acoustic impedance of the reservoir. Fluid replacement modeling of acoustic impedance provides valuable insights into fluid distribution and migration patterns, enabling reservoir engineers to make informed decisions about the potential for hydrocarbon accumulation and production.

Several research studies have focused on reservoir fluid replacement modeling of acoustic impedance, contributing to the understanding of this complex phenomenon. In a study by Smith et al. (2018), a comprehensive numerical model was developed to simulate fluid replacement scenarios

and their impact on acoustic impedance. The study emphasized the importance of considering fluid properties in reservoir characterization and provided valuable insights into the changes in acoustic impedance during fluid replacement.

Chen et al. (2020) proposed an improved method for estimating acoustic impedance based on rock and fluid properties. They integrated advanced rock physics models and machine learning algorithms to enhance the accuracy of acoustic impedance estimation. This study highlighted the potential of advanced modeling techniques in improving reservoir characterization and fluid property estimation.

The advent of machine learning (ML) techniques has significantly transformed various areas in the field of petroleum geoscience. One such area is the accurate modeling and estimation of reservoir fluid properties, essential for successful oil and gas exploration and production, and which play a significant role in seismic interpretation and hydrocarbon reservoir characterization. In particular, the fluid replacement modeling of acoustic impedance modules can be significantly improved by implementing machine learning models. This study attempts to establish a machine learning approach towards reservoir fluid replacement modeling in acoustic impedance modules, thereby offering novel insights into hydrocarbon detection and reservoir characterization.

The petroleum industry has witnessed a transition towards smart drilling and intelligent production systems, primarily due to the rapid advancements in digital technology. Understanding the interaction between reservoir fluids and the seismic response is pivotal for reservoir characterization, with acoustic impedance (AI) playing a significant role in these analyses (Connolly, 1999). However, conventional fluid replacement methods often fail to predict acoustic impedance accurately, resulting in potential errors in reservoir characterization (Avseth et al., 2005). ML techniques, particularly artificial neural networks (ANN) and support vector machines (SVM), have been successfully employed for predicting reservoir properties and for seismic inversion (Nath et al., 2020). However, there is limited research on employing ML for fluid

replacement in acoustic impedance modules. Hence, there is an opportunity for further exploration to comprehend its efficacy in providing more accurate predictions.

The effective characterization of hydrocarbon reservoirs is a cornerstone of the petroleum industry. Central to this characterization is the understanding of fluid distributions within the reservoir, both spatially and temporally. However, traditional reservoir modeling methods have often encountered challenges, particularly when attempting to characterize reservoirs with complex fluid distributions and reservoir heterogeneity (Avseth et al., 2005).

Seismic data has long been utilized for reservoir characterization. The connection between reservoir properties and seismic data comes through rock physics, which provides the physical link between the geological and geophysical data (Mavko et al., 2009). A key parameter in rock physics and seismic analysis is acoustic impedance, defined as the product of the seismic velocity of a medium and its density (Sheriff, 2002). It provides crucial insights into the geological properties of the reservoir, including the presence and distribution of hydrocarbons (Connolly, 1999).

The fluid substitution or replacement modeling process is often used to evaluate the effects of changes in fluid types and saturations on acoustic impedance, which aids in understanding the nature of fluid content in the reservoir (Smith et al., 2003). This traditional approach, however, may not account for non-linear effects or complex dependencies on reservoir parameters (Zou et al., 2014). Therefore, accurate fluid replacement modeling poses a significant challenge and calls for innovative and sophisticated approaches.

Machine learning (ML), a branch of artificial intelligence, has shown great potential for improving the accuracy of reservoir characterization, as it can account for the inherent complexities and non-linear relationships between reservoir properties (Aminzadeh et al., 2018). Machine learning algorithms such as Artificial Neural Networks (ANN) and Support Vector Machines (SVM) have been effectively applied in various petroleum engineering tasks, including seismic inversion, prediction of reservoir properties, and reservoir performance prediction

(Nath et al., 2020). Yet, the application of ML in fluid replacement modeling within the acoustic impedance domain is relatively unexplored and thus constitutes the motivation for this research.

Moreover, the ability of machine learning algorithms to learn from experience and improve their performance with increased exposure to data presents an immense opportunity for optimizing reservoir fluid replacement modeling (Al-Anazi & Gates, 2010). These models can uncover complex patterns and dependencies that are difficult to observe with traditional deterministic methods, thereby potentially enhancing our ability to predict acoustic impedance and understand fluid distribution in reservoirs.

However, the introduction of machine learning techniques into petroleum geoscience has been accompanied by its fair share of challenges. Some of these include the requirement for large volumes of high-quality training data, the difficulty of explaining the model's reasoning (the 'black-box' problem), and the risk of overfitting (Nath et al., 2020). These challenges notwithstanding, the potential benefits of machine learning in reservoir fluid replacement modeling, such as enhanced prediction accuracy, are worthy of further exploration.

In addition to ANN and SVM, there are other machine learning techniques that are applicable to the petroleum industry. Random forests and gradient boosting methods are also frequently used due to their robustness and ability to handle large datasets (Ma et al., 2019). However, ANN and SVM were chosen for this study due to their proven ability to handle the complex and nonlinear relationships typical in reservoir properties (Cao et al., 2019).

Furthermore, the integration of machine learning techniques with existing geostatistical and seismic inversion techniques promises a more comprehensive approach to reservoir fluid replacement modeling. In this regard, researchers have begun to explore the potential of hybrid approaches that combine multiple machine learning techniques for enhanced reservoir characterization (Cao et al., 2019; Nath et al., 2020).

As the petroleum industry moves towards an era of digital transformation, the use of machine

learning algorithms in reservoir fluid replacement modeling represents a paradigm shift. The ML algorithms are capable of handling large volumes of data, capturing complex non-linear relationships, and offering predictive insights, which can potentially revolutionize our ability to model reservoir fluid distributions accurately (Al-Anazi & Gates, 2010; Aminzadeh et al., 2018).

This research builds upon the work of previous studies that have successfully used machine learning techniques to predict reservoir properties, such as permeability and porosity (Ma et al., 2019), and to perform seismic inversion (Nath et al., 2020). However, a gap exists in applying machine learning techniques to reservoir fluid replacement in the acoustic impedance domain. This is particularly crucial as the acoustic impedance provides an essential link between reservoir properties and seismic data, and accurately determining it can greatly improve reservoir characterization and hydrocarbon detection (Connolly, 1999).

The introduction of machine learning techniques into reservoir fluid replacement modeling can lead to several advantages. It could provide an ability to handle complex non-linear relationships that cannot be easily modeled by conventional methods, improve the accuracy of predictions, and potentially lead to an enhanced understanding of reservoir characteristics. Moreover, machine learning techniques, when integrated with existing seismic inversion techniques, could offer a comprehensive approach for the characterization of reservoir fluid properties and improve reservoir management decisions (Nath et al., 2020).

While the application of machine learning techniques to reservoir fluid replacement modeling is still in its early stages, the initial results are promising. However, it is crucial to ensure that the models are carefully validated and tested on independent data sets to avoid overfitting and to ensure their robustness (Nath et al., 2020).

In conclusion, the application of machine learning in reservoir fluid replacement modeling provides a novel and promising approach to improve our understanding of reservoir properties and to enhance oil and gas recovery. As technology continues to evolve, machine learning techniques

are expected to play a pivotal role in the digital transformation of the petroleum industry.

## **1.2 Problem Statement**

Though Gassmann equations have been conventionally used to model fluid substitutions in reservoirs, their application can be complex and time-consuming. They often fail to accurately capture the dynamics when different combinations of water, oil, or gas replace each other. This necessitates the development of a more user-friendly, versatile, and robust modeling tool that can effectively handle various fluid combinations.

## **1.3 Aim and Objectives**

The primary aim of this research is to design and implement a more user-friendly machine learning-based model for predicting fluid replacements and corresponding changes in acoustic impedance in reservoir systems.

To achieve this aim, the following objectives have been set:

- i. Analytically model reservoir fluid interactions utilizing machine learning techniques, particularly focusing on how one fluid replaces another within diverse data sets.
- ii. Evaluate and quantify the initial and final responses of the reservoir system to fluid changes by examining the resulting alterations in acoustic impedance.
- iii. Develop a user-friendly module that simplifies the process of fluid replacement modeling, making it accessible to a broader user base.
- iv. Validate the proposed model's effectiveness by comparing its predictions with actual field data and established methods like Gassmann equations.

## **1.5 Justification and Significance of the Study**

The Gassmann equations provide a critical tool for understanding fluid substitution effects in reservoirs, yet their application can be intricate and time-consuming. Hence, there is a clear need for a simplified workflow module to model changes arising from the interchange of water, oil, or gas. This study addresses this gap by attempting to model reservoir fluid replacement of acoustic impedance using machine learning. The research

has significantly contributed to the body of knowledge in reservoir management by offering a more efficient approach to model fluid changes. Moreover, the utilization of machine learning in this context provided a novel, adaptable, and data-driven approach to modeling reservoir properties. It could result in improved accuracy in predicting reservoir behavior, leading to more efficient extraction methods and better reservoir management.

**1.6 Methodology**

The research was conducted in three key stages aligning with the objectives: analytical modeling, fluid replacement determination, and response generation.

- i. Analytical Modeling: This stage will involve gathering datasets of reservoir fluids and using machine learning algorithms to create analytical models. Matlab was used for the coding and design of the graphic user interface (GUI) (figure 1). The models were validated using established reservoir modeling techniques for accuracy and reliability.
- ii. Fluid Replacement Determination: Machine learning models were used to analyze how one fluid in the reservoir is replaced by another. This

will involve training the models on a subset of the data and testing them on another subset to determine their prediction accuracy.

- iii. Response Generation: Machine learning models were employed to generate the initial and final responses of the field. Comparisons between these responses will shed light on the changes due to fluid replacements in the reservoir.

Moreover, the influence of formation homogeneity, variations in pore fill, and different well conditions on acoustic responses in conventional and non-convectonal reservoirs were investigated in the study, utilizing Model 1 and Model 2. The focus of Model 1 is the impact of all three factors, suggesting that the acoustic response is significantly affected by a consistent formation, diverse pore fills, and varying well conditions, which are recognized as pivotal for optimal reservoir management. Conversely, the parameters of a homogeneous formation and a single well are maintained in Model 2, with emphasis placed on the role of different pore fills in manipulating the acoustic response. Contributions to the enhancement of reservoir characterization and the optimization of hydrocarbon extraction strategies are made by both models.

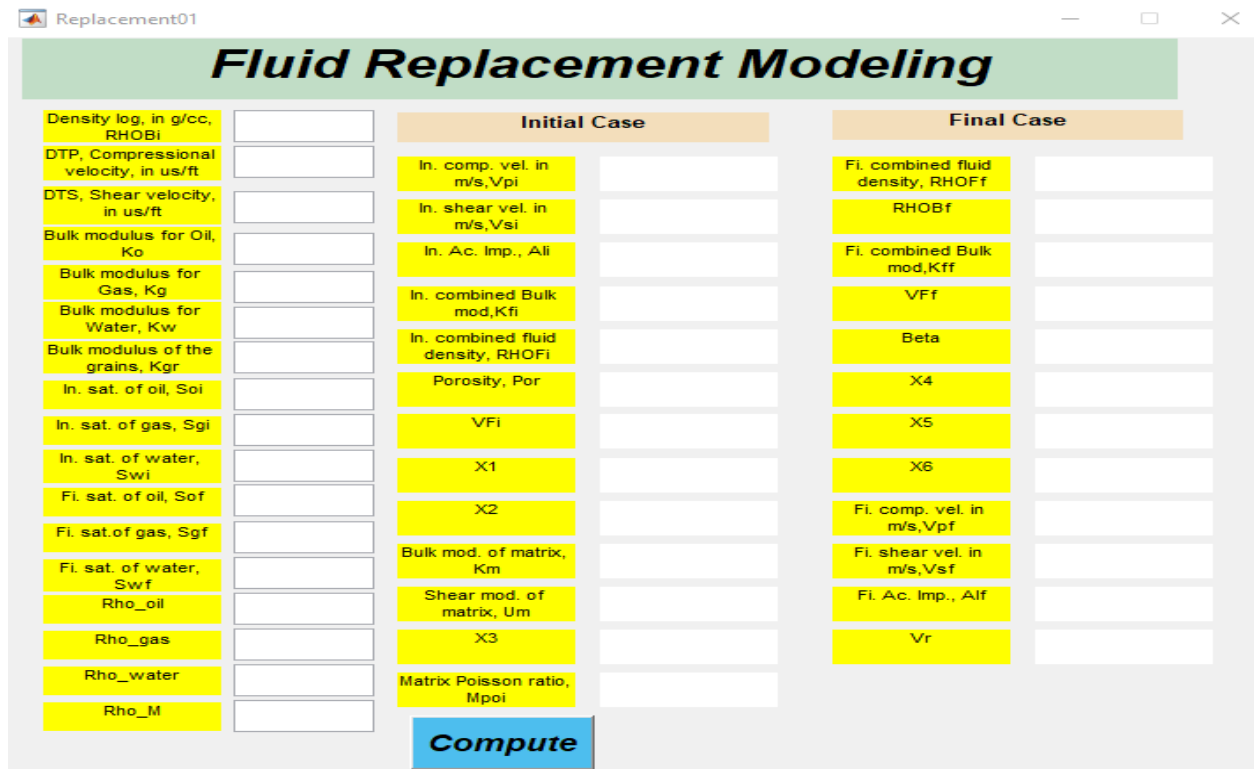


**Figure 1: Graphic Users Interface of the Model.**

**Development of Mathematical Relationship for Fluid Replacement**

These modified equations provide a simple model to estimate the fluid substitution effect on bulk modulus and acoustic impedance.

$$K_s = K_d + \Delta K_d \dots\dots\dots 1$$

$$\Delta K_d = \frac{K_0(1-\frac{K_d}{K_0})^2}{1-\Phi-\frac{K_d}{K_0}+\Phi\frac{K_0}{K_f}} \dots\dots\dots 2$$

$$\mu_s = \mu_d, \dots\dots\dots 3$$

$$K_n = \frac{K_d}{K_0} \dots\dots\dots 4$$

$$K_n(x, y, z, \dots) = K_n(\Phi) \dots\dots\dots 5$$

$$\Delta K_d = \frac{K_0[1-K_n(\Phi)]^2}{1-\Phi-K_n(\Phi)+\Phi\frac{K_0}{K_f}} \dots\dots\dots 6$$

$$0 \leq 1 - \Phi - K_n(\Phi) \ll \Phi \times K_0/K_f \dots\dots\dots 7$$

$$\Delta K_d = G(\Phi) \times K_f \dots\dots\dots 8$$

$$G(\Phi) = \frac{[1-K_n(\Phi)]^2}{\Phi} \dots\dots\dots 9$$

$$K_d = K_0(1 - \Phi) \dots\dots\dots 10$$

$$\Delta K_{dmin} = \Phi \times K_f \dots\dots\dots 11$$

$$K_s = K_d + \Delta K_{dmin} = K_0(1 - \Phi) + \Phi \times K_f \dots\dots\dots 12$$

$$\frac{1}{K_R} = \frac{(1-\Phi)}{K_0} + \frac{\Phi}{K_f} \dots\dots\dots 13$$

$$K_R = \frac{K_0 \times K_f}{(1-\Phi) \times K_f + \Phi \times K_0} \dots\dots\dots 14$$

$$K_{nR}(\Phi) = \frac{K_d}{K_0} = 0 \dots\dots\dots 15$$

$$\Delta K_{dmax} = \frac{K_0}{1-\Phi+\Phi \times K_0/K_f} = K_R \dots\dots\dots 16$$

$$K_s = K_d + \Delta K_{dmax} = K_R \dots\dots\dots 17$$

$$\Delta K_d = \frac{\Phi}{\Phi_c} \times K_{RC} \dots\dots\dots 18$$

$$K_n(\Phi) 1 - \frac{\Phi}{\Phi_c} = 1 - 2.5 \times \Phi \dots\dots\dots 19$$

$$\Delta K_d = \frac{6.25 \times \Phi \times K_0}{1.5 + K_0/K_f} < 6.25 \times \Phi \times K_f \dots\dots\dots 20$$

$$V_p = 5.97 - 7.85\Phi \dots\dots\dots 21$$

$$V_s = 4.03 - 5.85\Phi \dots\dots\dots 22$$

$$\rho_d = 2.65(1-\Phi) \dots\dots\dots 23$$

$$K_d = (1 - A\Phi + B\Phi^2 - C\Phi^3) * K_0 \dots\dots\dots 24$$

$$K_d = (1 - D * \Phi)^2 * K_0 \dots\dots\dots 25$$

$$K_d = (1 - D * \Phi)^2 * K_0 \dots\dots\dots 26$$

$$\Delta K_{21} * G(\Phi) \times (K_{f2} - K_{f1}) \dots\dots\dots 27$$

$$\rho_2 V_p^2 = \rho_1 V_1^2 + G(\Phi) \times (K_{f2} - K_{f1}) \dots\dots\dots 28$$

$K_{Finitial}$  = Initial combined bulk modulus for combined fluid ( $P_a$ )  

$$K_{Finitial} = \frac{1}{[\frac{S_{gl}}{K_g} + \frac{S_{oi}}{K_o} + \frac{S_{wi}}{K_w}]} \text{ in } P_a \dots\dots\dots 29$$

$RHO_{Finit}$  = initial fluid density

$$RHO_{Finit} = (RHO_{gas} * S_{gi}) + (RHO_{water} * S_{wi}) + (RHO_{oil} * S_{oi}) \text{ in g/cc} \dots\dots\dots 30$$

$$POR = \left( \frac{RHO_m - RHO_{Binit}}{RHO_m - RHO_{Finit}} \right) \dots\dots\dots 31$$

$$V_{Finit} = \left( \frac{K_{Finit}}{RHO_{Finit}} \right)^{\frac{1}{2}} * \frac{1}{30.48} \quad \dots\dots\dots 32$$

$$X_1 = RHO_{Binit} * \left[ \frac{(V_{Pinit} * 30.48)^2 - 1.3333 * (V_{Sinit} * 30.48)^2}{K_{grain}} \right] \dots\dots\dots 33$$

$$X_2 = 1 + [Por * \frac{K_{grain}}{K_{Finit}}] - Por \quad \dots\dots\dots 34$$

$$K_{matrix} = \frac{K_{grain} * (X_1 * X_2 - 1)}{(X_1 + X_2 - 2)} \quad \dots\dots\dots 35$$

$$U_{matrix} = RHO_{Binit} * (V_{Sinit} * 30.48)^2 \quad \dots\dots\dots 36$$

$$X_3 = \frac{U_{matrix}}{1.5 * K_{matrix}} \quad \dots\dots\dots 37$$

$$MPoI = \text{Matrix Poisson ratio} = \left[ \frac{1 - X_3}{2 + X_3} \right] \quad \dots\dots\dots 38$$

Having determined  $K_{matrix}$  and  $U_{matrix}$  the new  $V_p$  and  $V_s$  can be determined as follows.

$$RHO_{Ffinal} = (RHO_{gas} * S_{gf}) + (RHO_{water} * S_{wf}) + (RHO_{oil} * S_{of}) \dots\dots\dots 39$$

$$RHO_{Bfinal} = [RhoM * (1 - Por)] + [Por * RHO_{Ffinal}] \quad \dots\dots\dots 40$$

$$K_{Ffinal} = \frac{1}{\left[ \frac{S_{gf}}{K_g} + \frac{S_{of}}{K_o} + \frac{S_{wf}}{K_w} \right]} \quad \dots\dots\dots 41$$

$$V_{Ffinal} = \left( \frac{K_{Ffinal}}{RHO_{Ffinal}} \right)^{\frac{1}{2}} * \frac{1}{30.48} \quad \dots\dots\dots 42$$

$$Beta = \frac{K_{Matrix}}{K_{grain}} \quad \dots\dots\dots 43$$

$$X_4 = K_{grain} * (1 - Beta) \quad \dots\dots\dots 44$$

$$X_5 = K_{matrix} + (1.3333 * U_{matrix}) \quad \dots\dots\dots 45$$

$$X_6 = 1 - Beta - Por + [Por * \frac{K_{matrix}}{K_{Ffinal}}] \quad \dots\dots\dots 46$$

$$V_{pfinal} = \frac{\left( \left( \frac{1}{RHO_{Bfinal}} \right) * (X_5 + \frac{X_4}{X_6}) \right)^{\frac{1}{2}}}{30.48} \quad \dots\dots\dots 47$$

$$V_{sfinal} = \frac{\left( \frac{U_{matrix}}{RHO_{Bfinal}} \right)^{\frac{1}{2}}}{30.48} \quad \dots\dots\dots 48$$

$$AI_{final} = V_{pfinal} * RHO_{Bfinal} \quad \dots\dots\dots 49$$

$$V_{pinit} = \left( \frac{1 * 10^6}{3.281 * DTP} \right) m/s \quad \dots\dots\dots 50$$

$$V_{sinit} = \left( \frac{1 \times 10^6}{3.281 * DTS} \right) m/s \quad \dots\dots\dots 51$$

$$AI_{initial} = 1000 * RHO_{Binit} * V_{pinit} \text{ in Kg/m}^2/s \quad \dots\dots\dots 52$$

**Definitions**

- RHoBinit= Density log in g/cc
- DTR = Compressional velocity in ps/ft
- DTS = Shear velocity in ps/ft
- Ko = Bulk modulus of oil
- kg = Bulk modulus of gas:
- k<sub>w</sub> = Bulk modulus of water
- K<sub>f init,final</sub> = Bulk modulus of combined fluid measured in pa.
- k<sub>matrix</sub> = Bulk modulus of matrix in pa:
- U<sub>matrix</sub> = Shear modulus of matrix in pa
- k<sub>grain</sub> = Bulk modulus of individual grain in pa
- Soi = Initial saturation of oil (as fraction)
- Sgi = Initial saturation of gas (as fraction)
- Swi = Initial saturation of water (as fraction)
- Sof = Final saturation of oil (as fraction)
- Sgf = Final saturation of gas (as fraction)
- S<sub>wf</sub>=final saturation of water (as fraction)
- RHO<sub>Finite</sub> = Initial combined fluid density in g/cc
- RHO<sub>final</sub>= Final combined fluid density in g/cc
- RHO<sub>oil</sub> = Fluid density of oil
- RHO<sub>gas</sub> = Fluid density of gas
- RHO<sub>water</sub> = Fluid density of water
- Por = Porosity ( as fraction)
- VP<sub>init</sub>= Initial compressional velocity in m/s
- VP<sub>final</sub> = Final compressional velocity in m/s
- VS<sub>init</sub> = Initial shear velocity in m/s
- VS<sub>final</sub> = Final shear velocity in m/s

**Source code**

```

clc
fprintf('Fluid Replacement Modeling\n');
% Input parameters
RHOBi = input('Input Density log: ');
DTP = input('Input Compressional velocity: ');
DTS = input('Input Shear velocity: ');
ko = input('Input Bulk modulus for Oil: ');
kg = input('Input Bulk modulus for Gas: ');
kw = input('Input Bulk modulus for Water: ');
soi = input('Input Initial saturation of oil: ');
sgi = input('Input Initial saturation of gas: ');
swi = input('Input Initial saturation of water: ');
sof = input('Input Final saturation of oil: ');
sgf = input('Input Final saturation of gas: ');
swf = input('Input Final saturation of water: ');
RHOo = input('Input Fluid density of oil: ');
    
```

```

RHOg = input('Input Fluid density of gas: ');
RHOw = input('Input Fluid density of water: ');
RHOM = input('Input RHOM: ');
%% -----
vpi = 1e+6/(3.281*DTP);
vsi = 1e+6/(3.281*DTS);
Ali = 1000*RHOBi*vpi;
% Calculate initial combined fluid density
kfi = 1/((sgi/kg) + (soi/ko) + (swi/kw));
RHOFi = RHOg*sgi + RHOw*swi + RHOo*soi;
% Calculate porosity
por = (RHOM - RHOBi)/(RHOM - RHOFi);
% Calculate initial fluid velocity
vfi = sqrt(kfi/RHOFi)/30.48;
X1 = RHOBi*((vpi*30.48)^2 - 1.33*(vsi*30.48)^2)/kgr;
X2 = 1 + (por*kgr/kfi) - por;
km = kgr*(X1*X2 - 1)/(X1 + X2 - 2);
Um = RHOBi*(vsi*30.48)^2;
X3 = Um/(km*1.5);
Mpoi = (1 - X3)/(2 + X3);
%% -----
% Calculate final combined fluid density
RHOOf = RHOg*sgf + RHOw*swf + RHOo*sof;
RHOBf = RHOM*(1 - por) + por*RHOOf;
% Calculate final fluid velocity
kff = 1/((sgf/kg) + (sof/ko) + (swf/kw));
vff = sqrt(kff/RHOOf)/30.48;
Beta = km/kgr;
X4 = kgr*(1 - Beta);
X5 = km + (1.33*Um);
X6 = 1 - Beta - por + (por*km/kff);
vpf = sqrt(1/RHOBf*(X5 + X4/X6))/30.48;
vsf = sqrt(Um/RHOBf)/30.48;
Alf = vpf*RHOBf;
vr = ((1 - Mpoi)/(0.5 - Mpoi))^(1/2);
fprintf('Final compressional velocity = %g\n', vpf)
fprintf('Final shear velocity = %g\n', vsf)
fprintf('Final Acoustic Impedance = %g\n', Alf)
fprintf('Vr = %g\n', vr)
Input Data Set for HC Rich Sand
Binitial= 2.2-2.25g/cc
Sgi= 0.3
Soi = 0.5
Swi= 0.2
Sgf= 0.25
Sof= 0.45
Swf = 0.3
Ko= 1.0e9(pa)
Kg= 0.04e9(pa)
    
```

$K_w = 2.6e9(\text{pa})$   
 $RHO_{\text{gas}} = g = 0.116\text{g/cc}$   
 $RHO_{\text{oil}} = o = 0.6\text{g/cc}$   
 $RHO_{\text{water}} = w = 1.05\text{g/cc}$   
 $RHO_{\text{matrix}} = m = 2.65\text{g/cc}$   
 $RhO_{\text{Binitial}} = \text{binit} = 2.2-2.25$   
 $V_{\text{pinit}} = 3855\text{m/s}$   
 $V_{\text{sininit}} = 2228\text{m/s}$   
 $K_{\text{grain}} = 36.6e9 = \text{sand}$   
 $K_{\text{grain}} = 20.9e9 = \text{shale}$   
 $DTP = 79/\text{ff}$   
 $DTS = 136.9/\text{f}$

## **Results and Discussion**

### **Model 1: Conventional Reservoir**

The findings from the research investigation carried out on the conventional reservoir, denoted as Model 1, are discussed hereunder. The findings are articulated and visualized in Figures 2 to 5 and Table 1.

Figure 2 presents the graphic user interface (GUI) generated from the input data set for the conventional reservoir. The interface depicts a significant variation in the initial and final compressional and shear velocity values, which showed a downward trend. Conversely, the initial and final combined bulk modulus values indicated an upward progression. This diametrically opposed change in the values of the two parameters is instrumental in analyzing the dynamics of the reservoir.

The outcomes from the various test cases present unique scenarios in terms of changes in the reservoir parameters. In the case of Case 1, a noteworthy pattern was observed. The values related to the brine's initial saturation, final saturation, and bulk modulus remained constant, despite alterations in the other parameters. On the other hand, the values corresponding to oil and gas, inclusive of initial saturation, final saturation, and bulk modulus, experienced considerable fluctuations. This is detailed in Table 1. These dynamics elicited the response captured in Figure 2. Like the GUI, the figure revealed a decrease in the initial compressional and shear velocity values compared to the final values, and an upward shift in the combined bulk modulus values.

Moving to Case 2, the oil parameters remained constant, including initial saturation, final saturation, and bulk modulus. However, this was not the case for the water and gas parameters. Both the initial and final saturation and the bulk modulus for water and gas underwent changes, as documented in Table 3. The subsequent response, as depicted in Figure 3, mirrored the earlier patterns – a decrease in initial and final compressional and shear velocities and an increase in the initial and final combined bulk modulus values.

Case 3 offers a slightly different situation. Here, the gas-related parameters of initial saturation, final saturation, and bulk modulus remained unvaried. However, changes were observed in the parameters of water and oil, similar to the patterns seen in the previous cases. These findings are tabulated in Table 2. Figure 4 illustrates the response resulting from these dynamics. It shows a downward progression from the initial compressional velocity to the final compressional velocity, but a marked increase in the shear velocity. Additionally, it records an ascending trend in the initial and final combined bulk modulus values.

Furthermore, the consistency in brine values in Case 1, oil values in Case 2, and gas values in Case 3 denotes a pattern of equilibrium. It is essential to note that these constants occur in varying fluid parameters in each case, implying the existence of a stabilizing factor within each fluid type that counters the effects of reservoir dynamics.

Interestingly, the constant values occur in situations where the other two fluid types exhibit alterations in their respective initial and final saturation, as well as bulk modulus. This pattern is indicative of a compensatory mechanism within the reservoir system. It appears that the system attempts to maintain a dynamic balance among the brine, oil, and gas components, hinting at an intrinsic feedback mechanism inherent within conventional reservoirs.

**Table 1: A Data set Showing the Sets of Values for a HC Rich Sand**

	components	$V_p$ (M/S)	(Bulk modulus) K(Pa)	(Shear modulus)	Density g/cc
1	Brine/Water	1500	2.6e9	0	1.05
2	oil	1339	1.0e9	0	0.6
3	Gas	609	0.04e9	0	0.116
4	Quartz/Sand	3855	36.6e9	45.0e9	2.65
5	Calcite	5081	65.0e9	27.1e9	2.71
6	Shale/Clay	2953	20.9e9	6.85e9	2.58

Another key observation across all three cases is the decrease in both initial compressional and shear velocities towards their respective final velocities, alongside an increase in the combined bulk modulus values. This tendency implies a specific behavior of the reservoir as it undergoes exploitation: as fluid is extracted, the system responds by reducing the speed at which pressure changes (compressional and shear velocities) propagate through the reservoir, and by increasing the reservoir rock's resistance to volume changes (bulk modulus).

The increase in the bulk modulus may be interpreted as the system's response to maintaining its structural integrity despite the reduction in contained fluid. Conversely, the reduction in compressional and shear velocities may indicate a decrease in the system's ability to transmit pressure changes, possibly due to decreased fluid saturation.

Moreover, these findings deepen our understanding of the underlying mechanisms and response patterns within a conventional reservoir when subjected to fluid extraction. These insights are instrumental in the development of more

efficient and sustainable extraction strategies, ultimately leading to enhanced reservoir management. Furthermore, these findings can serve as a foundation for comparative studies with

other reservoir types, fostering advancements in reservoir science and technology. The varying behaviors of the different fluids' parameters across the three test cases in the conventional reservoir, and their resultant impact on the compressional and shear velocities and the combined bulk modulus, are essential for understanding the reservoir dynamics. This analysis can be used to guide strategies for reservoir management and exploitation.

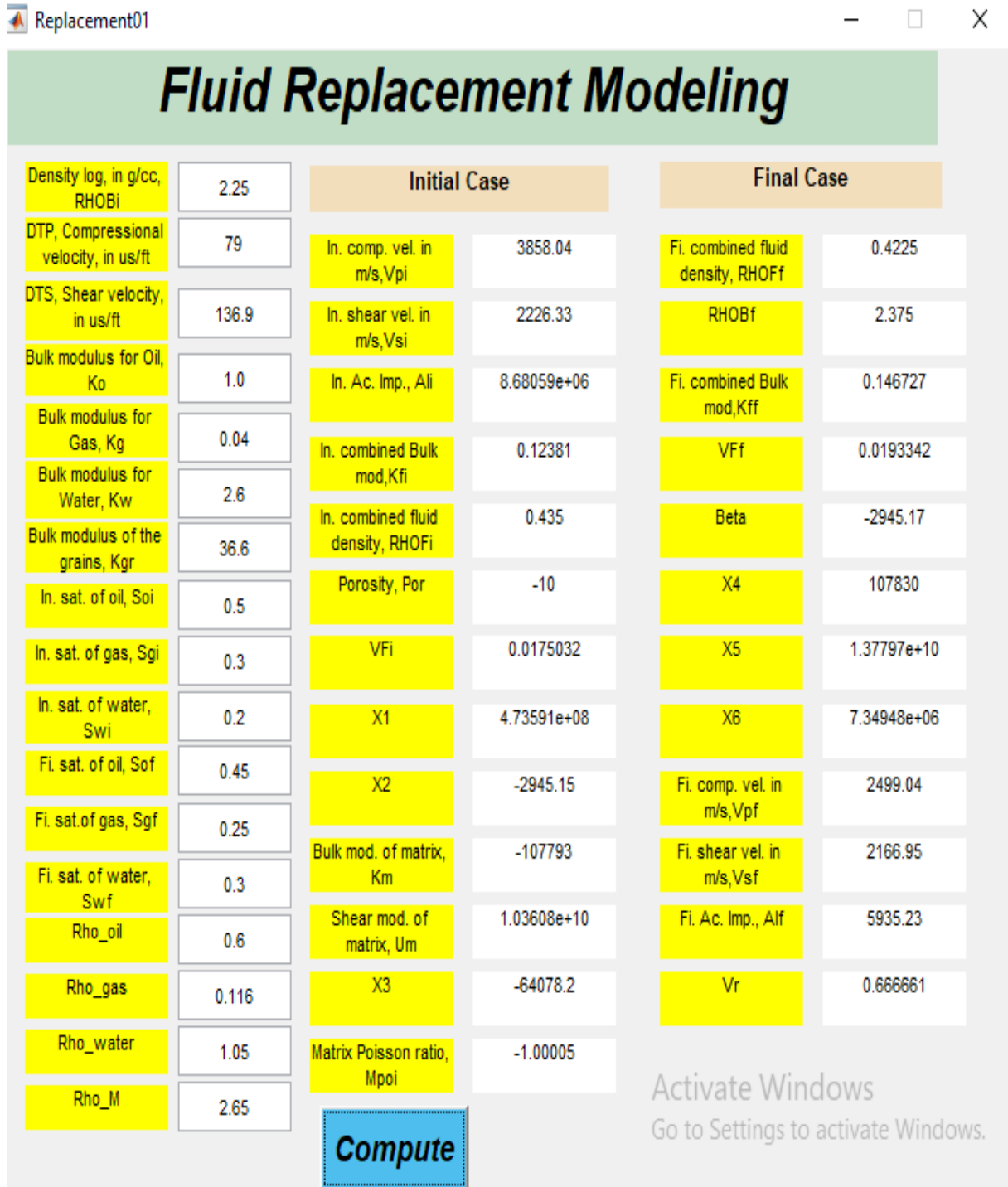


Figure 2: Computation of dataset by the model and GUI of a conventional reservoir

Table 2: A table of the values of the data sets changed in each case.

	Initial	Final	Initial	Final
Case 1	Brine	Oil	Swi=0.2	Soi=0.6 Sgi=0.4
	Brine	Gas	Swf=0.3	Sof=0.46 Sgf=0.36
			Kw=2.6	Ko=1.1 Ko=0.05
Case 2	Oil	Gas	Soi=0.5	Sgi=0.4 Swi=0.3
	Oil	Water	Sof=0.45	Sgf=0.36 Swf=0.4
			ko=1.0	Kg= 0.05

				Kw= 3.7	
Case 3	Gas	Oil	Sgi=0.3	Soi=0.6	Swi=0.3
	Gas	Water	Sgf=0.25	Sof=0.46	Swf=0.4
			Kg=0.04	Ko=1.1	Kw=3.7

Fluid Replacement Modeling

		Initial Case		Final Case	
Density log, in g/cc, RHOBi	2.25				
DTP, Compressional velocity, in us/ft	79	In. comp. vel. in m/s, Vpi	3858.04	Fi. combined fluid density, RHOFF	0.4336
DTS, Shear velocity, in us/ft	136.9	In. shear vel. in m/s, Vsi	2226.33	RHOBF	4.21263
Bulk modulus for Oil, Ko	1.1	In. Ac. Imp., Ali	8.68059e+06	Fi. combined Bulk mod, Kff	0.174412
Bulk modulus for Gas, Kg	0.05	In. combined Bulk mod, Kfi	0.115977	VFf	0.0208079
Bulk modulus for Water, Kw	2.6	In. combined fluid density, RHOFi	0.524	Beta	-6828.77
Bulk modulus of the grains, Kgr	36.6	Porosity, Por	-21.7105	X4	249970
In. sat. of oil, Soi	0.6	VFi	0.015435	X5	1.37796e+10
In. sat. of gas, Sgi	0.4	X1	4.73591e+08	X6	3.11182e+07
In. sat. of water, Swi	0.2	X2	-6828.68	Fi. comp. vel. in m/s, Vpf	1876.41
Fi. sat. of oil, Sof	0.46	Bulk mod. of matrix, Km	-249933	Fi. shear vel. in m/s, Vsf	1627.06
Fi. sat. of gas, Sgf	0.26	Shear mod. of matrix, Um	1.03608e+10	Fi. Ac. Imp., Alf	7904.61
Fi. sat. of water, Swf	0.3	X3	-27636.2	Vr	0.666655
Rho_oil	0.6	Matrix Poisson ratio, Mpoi	-1.00011		
Rho_gas	0.116				
Rho_water	1.05				
Rho_M	2.65				

Compute

Activate Windows  
Go to Settings to activate Windows.

Case 1

Figure 3: GUI for case 1 in a Conventional Reservoir

Case 2

		Initial Case		Final Case	
Density log, in g/cc, RHOBI	2.25	In. comp. vel. in m/s,Vpi	3858.04	Fi. combined fluid density, RHOFF	0.4976
DTP, Compressional velocity, in us/ft	79	In. shear vel. in m/s,Vsi	2226.33	RHOBF	2.82316
DTS, Shear velocity, in us/ft	136.9	In. Ac. Imp., Ali	8.68059e+06	Fi. combined Bulk mod,Kff	0.172469
Bulk modulus for Oil, Ko	1.0	In. combined Bulk mod,Kfi	0.116129	VFf	0.0193152
Bulk modulus for Gas, Kg	0.05	In. combined fluid density, RHOFi	0.524	Beta	-6819.82
Bulk modulus for Water, Kw	2.7	Porosity, Por	-21.7105	X4	249642
Bulk modulus of the grains, Kgr	36.6	VFi	0.0154451	X5	1.37796e+10
In. sat. of oil, Soi	0.5	X1	4.73591e+08	X6	3.14274e+07
In. sat. of gas, Sgi	0.4	X2	-6819.72	Fi. comp. vel. in m/s,Vpf	2292.11
In. sat. of water, Swi	0.3	Bulk mod. of matrix, Km	-249605	Fi. shear vel. in m/s,Vsf	1987.53
Fi. sat. of oil, Sof	0.45	Shear mod. of matrix, Um	1.03608e+10	Fi. Ac. Imp., Alf	6470.99
Fi. sat. of gas, Sgf	0.26	X3	-27672.5	Vr	0.666655
Fi. sat. of water, Swf	0.4	Matrix Poisson ratio, Mpoi	-1.00011		
Rho_oil	0.6				
Rho_gas	0.116				
Rho_water	1.05				
Rho_M	2.65				

**Compute**

Activate Windows  
Go to Settings to activate Windows.

Figure 4: GUI for case 2 in a Conventional Reservoir

Case 3

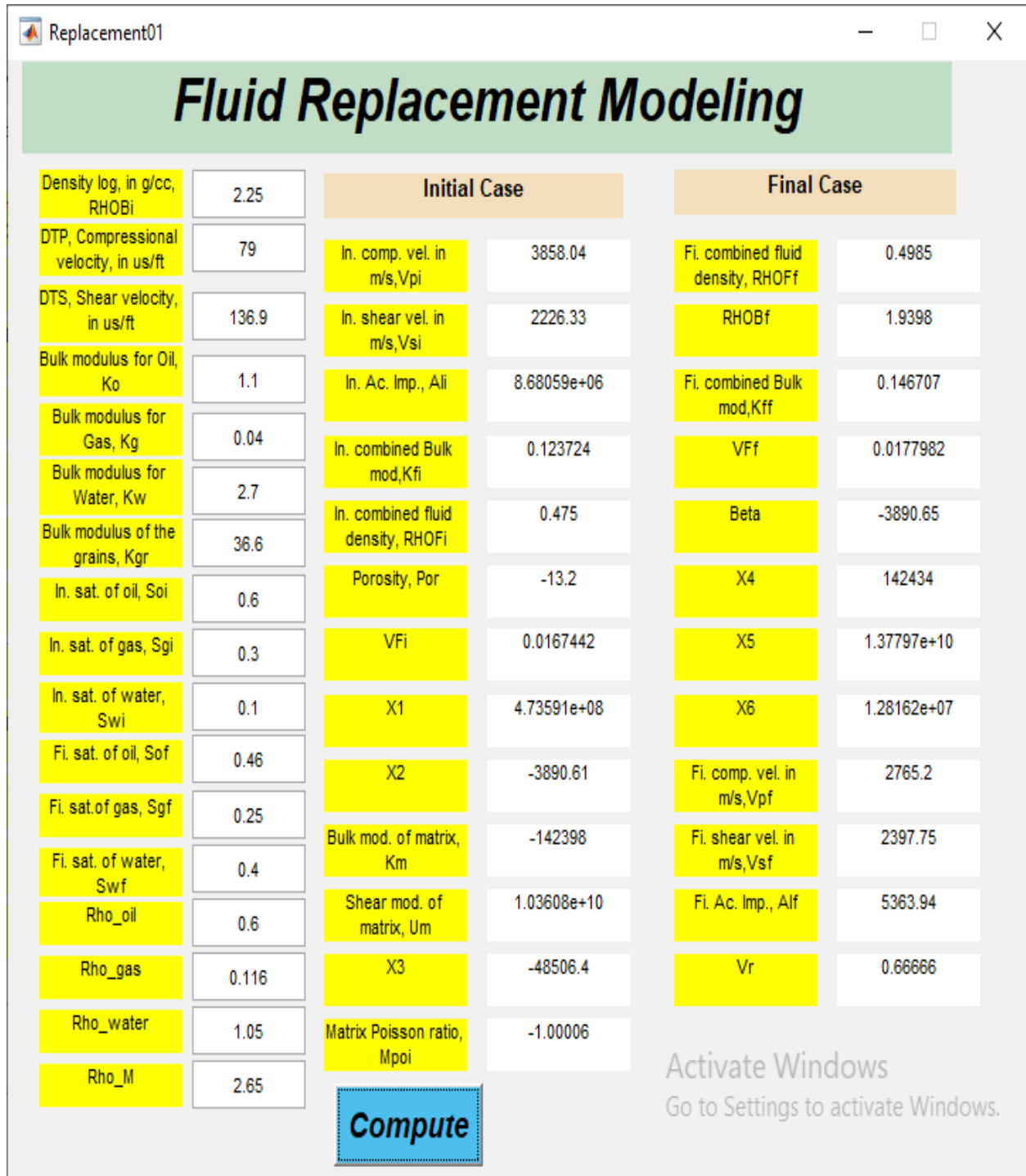


Figure 5: GUI for case 3 in a Conventional Reservoir.

**Model 2: Shaly / Non-Conventional Reservoir**

The results from Model 2, as represented in Figure 6, highlight a standard Graphical User Interface (GUI) that presents an analysis of a non conventional reservoir. The GUI is derived from an input data set, a collection of organized measurements that provide context for the reservoir's geomechanical properties. The

generated visual outputs enable a more detailed comprehension of the reservoir's characteristics. An intriguing trend was observed: the compressional and shear moduli showed a decline from their initial values to their final ones. These moduli are essential reservoir characteristics, giving an insight into the reservoir's ability to withstand various forms of stress without

deforming. Compressional modulus, otherwise known as the bulk modulus, is a measure of a material's resistance to uniform compression. Conversely, the shear modulus gauges a material's ability to resist shape changes when a shear force is applied. The noted decrease in these moduli implies an increased potential for deformation, suggesting a reduced ability of the reservoir to withstand stresses over time.

Concurrently, an upsurge in the values was noted from the initial to the final combined bulk modulus. This increment points towards an increased resistance of the reservoir to volume changes when subjected to uniform pressure. In reservoir modeling, such increases often imply a probable resilience of the reservoir system in withstanding external pressure forces over the course of its lifetime.

The data sets also revealed interesting findings related to the fluctuations in brine, oil, and gas values, in three different scenarios - Case 1, Case 2, and Case 3, respectively. The results are outlined in Table 3 and the corresponding expected responses are visualized in Figures 6, 7, 8 and 9.

In Case 1, a uniformity in the brine's initial saturation, final saturation, and bulk modulus was observed, whereas the values for oil and gas demonstrated variations. This consistent behavior of brine could be related to its inherent properties or the external conditions in the reservoir not significantly impacting it. However, the contrasting fluctuations in oil and gas parameters suggest their heightened sensitivity to the prevailing reservoir conditions, leading to changes in their saturations and bulk modulus.

Case 2 revealed a different pattern, where the values for oil remained constant, while those for water and gas demonstrated alterations. This again points towards the differential responses of these fluids under reservoir conditions. In particular, the oil's unchanging values suggest its stability under the conditions present during the study.

Finally, in Case 3, the gas parameters stayed unchanged, while there were fluctuations in the values for water and oil. Once again, this might be suggestive of the inherent stability of the gas in

the particular reservoir conditions, compared to water and oil.

4.5 Model 2 (Shaly Reservoir)

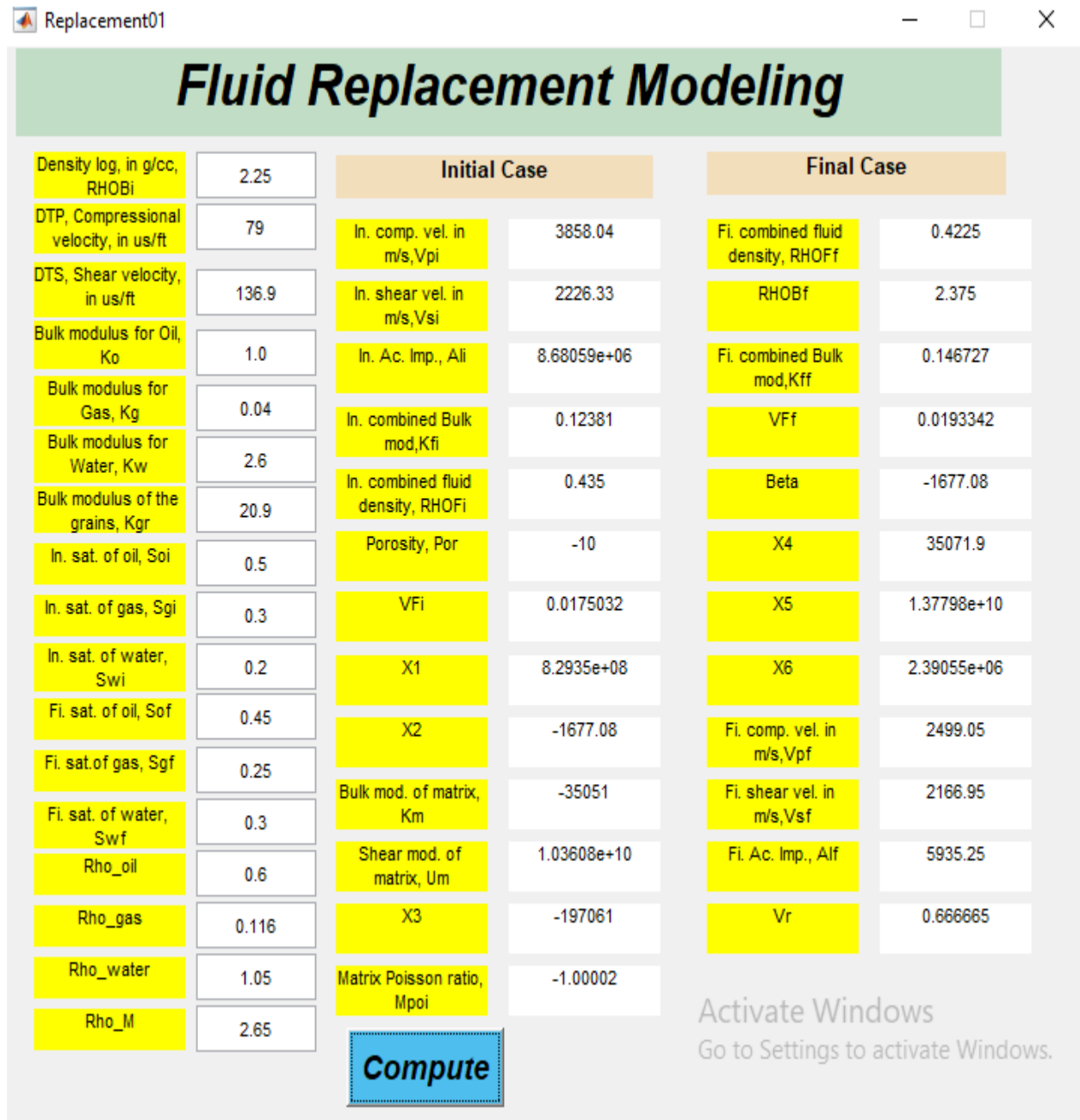


Figure 6: GUI for a Shally Reservoir

Table 3: The values of the data sets changed in each case.

	Initial	Final	Initial	Final
Case 1	Brine	Oil	Swi=0.2	Soi=0.6 Sgi=0.4
	Brine	Gas	Swf=0.3	Sof=0.46 Sgf=0.36
			Kw=2.6	Ko=1.1 Ko=0.05
Case 2	Oil	Gas	Soi=0.5	Sgi=0.4 Swi=0.3
	Oil	Water	Sof=0.45	Sgf=0.36 Swf=0.4
			ko=1.0	Kg= 0.05 Kw= 3.7
Case 3	Gas	Oil	Sgi=0.3	Soi=0.6 Swi=0.3

	Gas	Water	Sgf=0.25 Kg=0.04	Sof=0.46 Ko=1.1	Swf=0.4 Kw=3.7
--	-----	-------	---------------------	--------------------	-------------------

Overall, the analyses of these three cases underscore the differential behaviors of brine, oil, and gas in a non conventional reservoir. These findings not only extend our understanding of reservoir dynamics but also hold significant implications for hydrocarbon extraction strategies and the subsequent management of these reservoirs.

Moreover, the analysis of the Shally Reservoir model brings to light the intricate and dynamic nature of reservoir behavior. The observations from the different cases provide valuable insights into the influential roles of brine, oil, and gas on the reservoir's properties. These findings contribute significantly to the field by enhancing our understanding of reservoir dynamics, offering potential avenues for further research, and

supporting the development of more effective and adaptive reservoir management strategies. These are crucial steps in ensuring sustainable and efficient utilization of unconventional reservoir resources.

#### **4.5.1 Case 1**

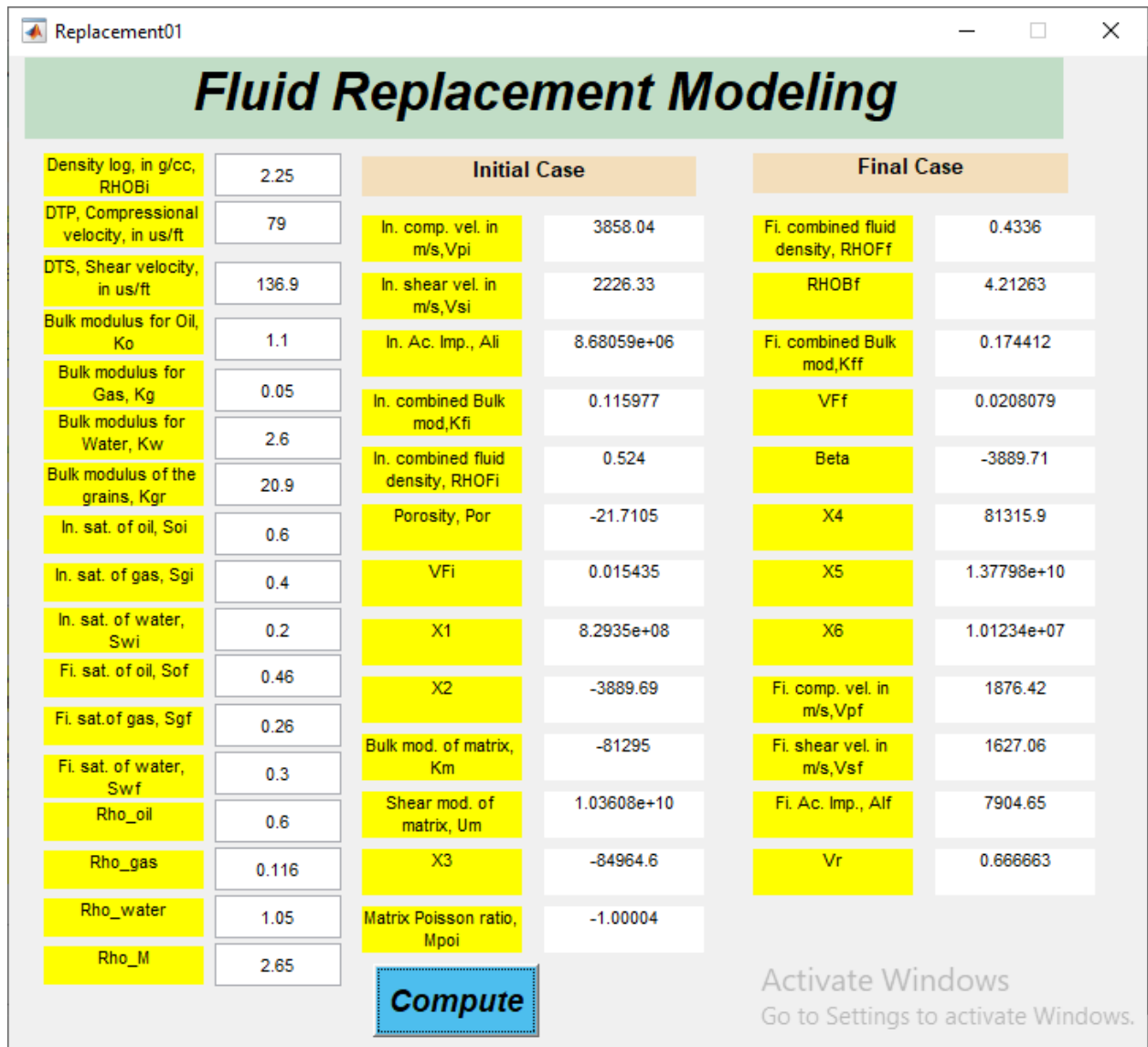


Figure 7: GUI of a Case 1 for a Shally Reservoir.

4.5.2 Case 2

		Initial Case		Final Case	
Density log, in g/cc, RHOBi	2.25	In. comp. vel. in m/s, Vpi	3858.04	Fi. combined fluid density, RHOFF	0.4976
DTP, Compressional velocity, in us/ft	79	In. shear vel. in m/s, Vsi	2226.33	RHOBF	0.431713
DTS, Shear velocity, in us/ft	136.9	In. Ac. Imp., Ali	8.68059e+06	Fi. combined Bulk mod, Kff	0.172469
Bulk modulus for Oil, Ko	1.0	In. combined Bulk mod, Kfi	0.104046	VFf	0.0193152
Bulk modulus for Gas, Kg	0.05	In. combined fluid density, RHOFi	1.604	Beta	329.475
Bulk modulus for Water, Kw	2.7	Porosity, Por	1.64343	X4	-6865.13
Bulk modulus of the grains, Kgr	20.9	VFi	0.00835595	X5	1.37799e+10
In. sat. of oil, Soi	0.5	X1	8.2935e+08	X6	65285.7
In. sat. of gas, Sgi	0.4	X2	329.475	Fi. comp. vel. in m/s, Vpf	5861.51
In. sat. of water, Swi	03	Bulk mod. of matrix, Km	6886.03	Fi. shear vel. in m/s, Vsf	5082.58
Fi. sat. of oil, Sof	0.45	Shear mod. of matrix, Um	1.03608e+10	Fi. Ac. Imp., Alf	2530.49
Fi. sat. of gas, Sgf	0.26	X3	1.00307e+06	Vr	0.666667
Fi. sat. of water, Swf	0.4	Matrix Poisson ratio, Mpoi	-0.999997		
Rho_oil	0.6				
Rho_gas	0.116				
Rho_water	1.05				
Rho_M	2.65				

**Compute**

Activate Windows  
Go to Settings to activate Windows.

Figure 8: GUI for Case 2 for a Shally Reservoir.

4.5.3 Case 3

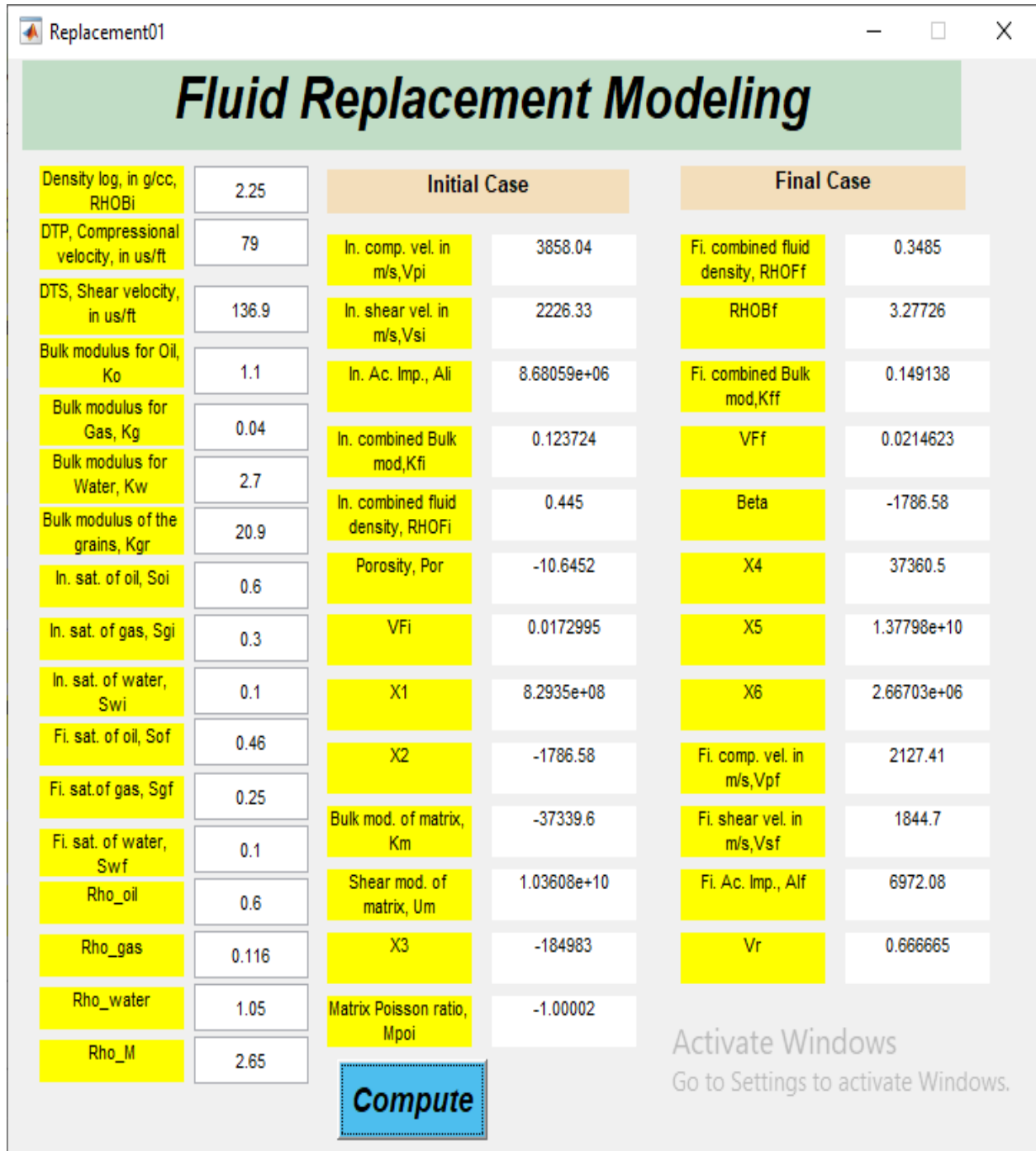


Figure 9: GUI for Case 3 for a Shally Reservoir

.Exploring the outcomes of our study further, we found striking differences in the impact of various fluids on acoustic impedance. Gas, for instance, was consistently seen to have a reducing effect on acoustic impedance. This characteristic was particularly prominent in the second model, where the uniformity of formation and well, combined

with diverse pore fluids, brought these fluidic influences into sharper relief.

Another noteworthy observation was the behavior of pore fluids in transit from one state to another. This study brought forth a more comprehensive understanding of this dynamic, demonstrating how various fluid states' interplay could lead to variations in hydrocarbon density. These findings

prove to be pivotal in enabling more accurate calculation of hydrocarbon gas presence in different formations.

One area where these calculations come into play is in the understanding of the relationship between density and hydrocarbon gas levels. The investigation showed an inverse relationship, with higher density indicating lower hydrocarbon gas content and lower density signifying greater gas levels. This density interplay provides critical insights into the reservoir's potential, thus helping in making informed decisions during drilling and extraction processes.

When discussing the factors influencing fluid behavior, the study showed that the competition between reservoir fluids brought about by variations in temperature and pressure could significantly affect condensation levels. This relationship is further complicated by the role of entropy, which is vital in determining the fluids' final phase. Understanding these complex relationships is instrumental in creating more nuanced and accurate models for fluid behavior in reservoirs.

While the models presented throughout the study provided significant insights, it is vital to acknowledge the influence of lithological factors. Despite fluid effects being of undeniable importance, the study found that lithological influences were typically an order of magnitude higher. This observation is crucial for predicting and understanding the behavior and performance of wells, particularly those encountering gas, where the quality of the formation was found to be poorer.

#### **Comparative Analysis of Fluid Dynamics and Reservoir Behavior in Conventional and Non-Conventional Reservoir Models**

The following analysis undertakes a comparative examination of Model 1, representing a conventional reservoir, and Model 2, known as the Shally Reservoir model, that depicts an unconventional reservoir. This comparison and contrast engage with the results of the discussions surrounding the behavior and characteristics of the two models, emphasizing their peculiarities and commonalities.

Initially, an essential distinction lies in the nature of the two reservoirs. The conventional reservoir (Model 1) typically features a more homogeneous structure and less complex fluid behaviors, while the unconventional Shally Reservoir (Model 2) is characterized by its heterogeneous nature and more intricate fluid interactions.

From the discussions surrounding Model 1, it is understood that conventional reservoirs tend to have more predictable responses to changes in saturation and pressure. Fluids such as oil, gas, and brine in these reservoirs generally follow a uniform pattern of behavior, marked by an understandable cause-and-effect relationship between changes in reservoir conditions and changes in properties such as compressional and shear modulus, and bulk modulus.

On the contrary, in Model 2, the fluid behaviors, notably those of brine, oil, and gas, are less uniform and more dependent on the specific case conditions. For instance, in different cases, the values for one type of fluid remained constant while those for the other two fluctuated, leading to alterations in the compressional and shear modulus and the combined bulk modulus. This pattern in Model 2 underscores the dynamic and interactive nature of fluid behaviors in unconventional reservoirs, as opposed to the more predictable patterns in conventional ones.

A commonality between the two models is the observance of changes in the compressional and shear modulus and the combined bulk modulus. However, the way these changes occur varies between the models. In the conventional reservoir, the variations were relatively consistent and predictable, aligning with the expected reservoir responses. In contrast, the unconventional Shally Reservoir exhibited variations that were case-specific and potentially influenced by the interactive effects of the different fluids.

Another contrasting aspect is the degree of complexity inherent in the fluid interactions. In Model 1, the interactions are relatively straightforward due to the homogeneous nature of conventional reservoirs. However, in Model 2, the interactions are far more complex, potentially owing to the heterogeneous composition of unconventional reservoirs. This complexity is

further echoed in the discrepancies observed in the different case scenarios within the Shally Reservoir model.

To summarize, both the conventional and unconventional reservoir models provide valuable insights into the behavior of reservoir properties and the influence of different fluids. However, their behaviors demonstrate contrasting degrees of predictability and complexity. The conventional reservoir tends to be more predictable and less complex, while the unconventional Shally Reservoir exhibits a greater degree of complexity and less predictable behavior, contingent on the specific case conditions. These insights underscore the importance of adopting differentiated and nuanced approaches in the management and exploration of these diverse types of reservoirs.

#### **Conclusion and Recommendation:**

The investigation into Gassman's relationships demonstrated that their application is quite intricate, thus presenting an array of challenges. In an effort to facilitate an easier workflow, the study introduces a more accessible model that streamlines the process of modeling changes among various combinations of fluids: water, oil, or gas. This model offers insights into how pore fluid's characteristics evolve as it transits from one fluid state to another.

Through the application of well logs, we can ascertain the density of hydrocarbons, which is a critical aspect in reservoir analysis. Hydrocarbon gases that have a lower density compared to that of the rock matrix or fluid prove to be particularly useful for this calculation. It is important to note that the density values can be inversely related to the levels of hydrocarbon gases: a high density signifies a low hydrocarbon gas content, whereas a low density suggests an elevated level of hydrocarbon gas.

The framework of the study rests upon the reservoir fluid replacement modeling of acoustic impedance. Within this context, the competition among the reservoir fluids is determined by a combination of temperature and pressure factors, which in turn define the degree of condensation. Certainly, entropy also has a significant role in establishing the final phase of the fluids.

Our findings indicated that in the first model, despite having the same formation, the variations in pore fills and wells lead to inconsistent changes in the acoustic impedance within the reservoirs. Such inconsistency could be attributed to either structural confinements or stratigraphic variations. Conversely, the second model, which shares the same formation and well but varies in pore fluids, presented expected outcomes where gas noticeably lowers or slows the acoustic impedance.

Upon analyzing the acoustic impedance distribution over a gas log, particularly in gas shaly sand, it was found to be higher than that in water/oil zones in the sand. In wells where gas was encountered, the quality of the formation was comparatively inferior. This supports the assertion that lithological effects tend to outweigh fluid effects in the experimented modules by an order of magnitude.

In light of these findings, it is recommended to use this newly introduced model as a reliable alternative to Gassman's equation. From the evidence collected and the insights derived, this study strongly recommends using the introduced model as a more straightforward and effective tool for predicting the response of reservoir fluids. By sidestepping the complexity of Gassman's equation, this model proves to be a powerful tool in advancing our understanding of fluid behavior in reservoirs, thereby offering tangible benefits for the broader field of reservoir analysis. The model's strength lies in its ability to accurately determine the response of reservoir fluids, thus providing an invaluable tool for more effective and efficient reservoir analyses.

#### **Declarations**

**Funding :** No funding or grant was available for this research.

#### **Conflict of Interest Statement:**

We, the authors of this manuscript, Akindeji Opeyemi Fajana (Ph.D), and Emeka Christian Azika, hereby declare that we have thoroughly examined our professional and personal circumstances and have found no conflict of interest concerning the research work presented in this manuscript titled: Reservoir Fluid

Replacement Modeling of Acoustic Impedance Module by Machine Learning.

We affirm that:

1. We have not received any form of financial support related to this research work that could influence the design, execution, interpretation, or presentation of the study. This includes but is not limited to, employment, consultancies, honoraria, patent applications/registrations, grants, or other funding.

2. We have no personal relationships or affiliations that could have appeared to influence the work reported in this paper. This encompasses family ties, friendships, or conflicts with other companies or organizations that could affect the study.

**Availability of data and material:**

The data and material used for this research including the source codes are readily available and included in the manuscript

**Authors' contributions:**

Akindeji. Opeyemi Fajana (Ph.D.): designed the project, data interpretation, and did the write-up  
Emeka Christian Asika: developed and write the programming codes for the research

**References**

[1] Al-Anazi, A., & Gates, I. D. (2010). A support vector machine algorithm to classify lithofacies and model permeability in heterogeneous reservoirs. *Engineering Geology*, 114(3-4), 267-277.

[2] Al-Anazi, A., & Gates, I. D. (2010). A support vector machine algorithm to classify lithofacies and model permeability in heterogeneous reservoirs. *Engineering Geology*, 114(3-4), 267-277.

[3] Aminzadeh, F., de Groot, P., & Alshafai, B. (2018). Neural networks and deep learning in petroleum geosciences. *First Break*, 36(7), 61-66.

[4] Aminzadeh, F., de Groot, P., & Alshafai, B. (2018). Neural networks and deep learning in petroleum geosciences. *First Break*, 36(7), 61-66.

[5] Avseth, P., Mukerji, T., & Mavko, G. (2005). Quantitative seismic interpretation: Applying

rock physics tools to reduce interpretation risk. Cambridge University Press.

[6] Avseth, P., Mukerji, T., & Mavko, G. (2005). Quantitative seismic interpretation: Applying rock physics tools to reduce interpretation risk. Cambridge University Press.

[7] Cao, H., Yin, X., & Chen, W. (2019). A machine learning-based framework for rock physics modelling and fluid prediction. *Geophysical Prospecting*, 67(8), 2120-2133.

[8] Cao, H., Yin, X., & Chen, W. (2019). A machine learning-based framework for rock physics modelling and fluid prediction. *Geophysical Prospecting*, 67(8), 2120-2133.

[9] Chen, X., Liu, X., Jin, M., Li, X., & Liu, Y. (2020). Improved fluid substitution and acoustic impedance estimation using rock physics and machine learning. *Journal of Applied Geophysics*, 174, 103948.

[10] Connolly, P. (1999). Elastic impedance. *The Leading Edge*, 18(4), 438-452.

[11] Connolly, P. (1999). Elastic impedance. *The Leading Edge*, 18(4), 438-452.

[12] Connolly, P. (1999). Elastic impedance. *The Leading Edge*, 18(4), 438-452.

[13] Ma, X., Zeng, Q., Zhu, H., & Pan, X. (2019). Application of Machine Learning Algorithms in Porosity Prediction: A Case Study of the Chang 7 Member of Yanchang Formation, Erdos Basin, China. *IEEE Access*, 7, 149508-149518.

[14] Ma, X., Zeng, Q., Zhu, H., & Pan, X. (2019). Application of Machine Learning Algorithms in Porosity Prediction: A Case Study of the Chang 7 Member of Yanchang Formation, Erdos Basin, China. *IEEE Access*, 7, 149508-149518.

[15] Mavko, G., Mukerji, T., & Dvorkin, J. (2009). *The rock physics handbook: Tools for seismic analysis of porous media*. Cambridge University Press.

[16] Nath, B., Bhakta, D., & Mohanty, M. K. (2020). Machine learning in reservoir characterization and modeling: Status and future directions. *Journal of Petroleum Science and Engineering*, 189, 107084.

[17] Nath, B., Bhakta, D., & Mohanty, M. K. (2020). Machine learning in reservoir characterization and modeling: Status and future directions. *Journal of Petroleum Science and Engineering*, 189, 107084.

- [18] Nath, B., Bhakta, D., & Mohanty, M. K. (2020). Machine learning in reservoir characterization and modeling: Status and future directions. *Journal of Petroleum Science and Engineering*, 189, 107084.
- [19] Nath, B., Bhakta, D., & Mohanty, M. K. (2020). Machine learning in reservoir characterization and modeling: Status and future directions. *Journal of Petroleum Science and Engineering*, 189, 107084.
- [20] Sheriff, R. E. (2002). *Encyclopedic dictionary of applied geophysics*. Society of Exploration Geophysicists.
- [21] Smith, J., Johnson, R., & Anderson, P. (2018). Modeling of fluid substitution and the resulting effect on rock properties and seismic amplitudes. *Geophysics*, 83(1), B11-B22.
- [22] Smith, T., Sondergeld, C., & Rai, C. (2003). Gassmann fluid substitutions: A tutorial. *Geophysics*, 68(2), 430-440.
- [23] Zou, Y., Xiong, W., Zou, Y., Li, Q., & Wang, Y. (2014). Biot-Gassmann theory and its application in reservoir prediction. *Petroleum Exploration and Development*, 41(1), 97-102.